A Simple model for NN correlations in quasielastic lepton-nucleus scattering

A simple model for NN correlations in quasielastic lepton-nucleus scattering

M.B. Barbaro[1], R. Cenni[2], T.W. Donnelly[3], and A. Molinari[1]

[1] Università di Torino and INFN, Sezione di Torino, Italy
[2] INFN, Sezione di Genova, Italy
[3] CTP, LNS and Department of Physics, MIT, Cambridge, USA

Abstract. We present a covariant extension of the relativistic Fermi gas model which incorporates correlation effects in nuclei. Within this model, inspired by the BCS descriptions of systems of fermions, we obtain the nuclear spectral function and from it the superscaling function for use in treating high-energy quasielastic electroweak processes. Interestingly, this model has the capability to yield the asymmetric tail seen in the experimental scaling function.

1 Introduction

Recently the theoretical understanding of quasielastic (QE) lepton-nucleus scattering has received renewed attention not only because of its intrinsic interest but also because reliable calculations of neutrino-nucleus cross section in the QE domain are essential when addressing fundamental neutrino properties, specifically neutrino masses and the neutrino oscillations that result from those masses.

In particular it has been suggested [1] that superscaling [2, 3] in electroweak interactions with nuclei, namely the observation that the reduced electron-nucleus cross sections are to a large degree independent of the momentum transfer (scaling of I kind) and of the nuclear species (scaling of II kind), can be used as a tool to obtain predictions for neutrino-nucleus cross sections. Owing to the complexity of nuclear dynamics it is not obvious that the nuclear response to an electroweak field superscales. Indeed several effects are expected to break superscaling to some extent: off-shellness, collective nuclear excitations, meson-exchange currents, nucleon-nucleon (NN) correlations. To assess the impact of these contributions in the QE peak region is then of crucial importance.

In the present work we explore the role of NN correlations in the QE peak domain proposing an extension of the Relativistic Fermi Gas (RFG) approach which still includes only on-shell nucleons in an independent-particle model, and put our efforts into going beyond the degenerate description provided by the extreme RFG. To do this we resort to a model [4] inspired by the BCS theory of condensed matter physics with appropriate modifications, such as retention of covariance, to adapt it to the high-energy physics of atomic nuclei.

2 Longitudinal response and superscaling function

We concentrate here on the longitudinal electromagnetic nuclear response R_L, namely the part of the total inclusive electroweak response that is believed to superscale the best [3]. All other electroweak responses can be developed using similar arguments to those presented in the following. Within the framework of the plane-wave impulse approximation, where it is assumed that only one vector boson is exchanged between the probe and the nucleus and that this one is absorbed by a single nucleon, the QE longitudinal response function of a nucleus to an external electroweak field bringing three-momentum $\mathbf{q}$ and energy ω into the system reads

$$R_L(q,\omega) = \mathcal{N}\, R_L^{s.n.}(q,\omega)\, \frac{2\pi m_N^2}{q} \iint_\Sigma dp\, d\mathcal{E}\, \frac{p}{E_p} S(p,\mathcal{E})\,, \tag{1}$$

where $\mathcal{N}$ is the appropriate nucleon number (Z for protons and N for neutrons), $R_L^{s.n.}(q,\omega)$ is the corresponding single nucleon response and $E_p = \sqrt{p^2+m_N^2}$ is the on-shell energy of the struck nucleon, with m_N the nucleon mass. The probability of finding one nucleon in the system is provided by the system's spectral function $S(p,\mathcal{E})$, which depends on the missing momentum p and on the energy

$$\mathcal{E} = \sqrt{p^2 + M_{A-1}^{*2}} - \sqrt{p^2 + M_{A-1}^2} = \omega - T_N - E_s - T_{A-1}\,. \tag{2}$$

The latter is the excitation energy of the residual nucleus in the reference frame where it moves with momentum $-\mathbf{p}$ and, neglecting the very small recoiling nucleus kinetic energy T_{A-1}, is essentially the missing energy $\omega - T_N$, T_N being the ejected nucleon kinetic energy, minus the separation energy $E_s = M_{A-1} + m_N - M_A$.

Equation (1) connects the semi-inclusive $(l,l'N)$ reaction with the inclusive (l,l') process assuming that the outgoing nucleon no longer interacts with the residual $(A-1)$ nucleus (absence of final-state interactions). That equation expresses the assumption that the inclusive cross section is to be obtained by integrating the semi-inclusive cross section, summing over struck protons and neutrons. The boundaries of the integration domain Σ in the $(\mathcal{E},p)$ plane are found through the energy conservation relation (see [4, 5] for the explicit expressions).

A further approximation underlies (1), namely the factorization of the single-nucleon response $R_L^{s.n.}(q,\omega)$ out of the integral. Actually this response is in general half-off-shell and hence a function not only of q and ω, but also of the energy and momentum of the off-shell struck nucleon, or equivalently of p and $\mathcal{E}$. In the models being considered in the present study the struck nucleon is in fact on-shell and so $R_L^{s.n.}$ becomes simply the longitudinal response of a moving free nucleon. In this case its dependence upon p and $\mathcal{E}$ becomes very weak, particularly if one limits the focus only to regions where the spectral function $S(p,\mathcal{E})$ plays a significant role, and can accordingly be extracted from the integral.

Finally, in this study we confine ourselves to dealing with infinite, homogeneous systems, the simplest among them being the RFG model in which the dynamics are controlled by just one parameter, the Fermi momentum k_F. To explore superscaling it then turns out to be convenient to recast (1) in the following form

$$R_L(q,\omega) = \mathcal{N}\, R_L^{s.n.}(q,\omega)\, \Lambda \times f(q,\omega)\,, \tag{3}$$

where

$$\Lambda = \frac{1}{k_F}\left(\frac{m_N}{q}\right)\left(\frac{2m_N T_F}{k_F^2}\right) \simeq \frac{m_N}{k_F q}\,, \tag{4}$$

T_F being the Fermi kinetic energy. The function

$$f(q,\omega) = 2\pi m_N k_F \times \frac{k_F^2}{2m_N T_F} \iint_\Sigma dp\, d\mathcal{E}\, \frac{p}{E_p} S(p,\mathcal{E})\,, \tag{5}$$

is the so-called *superscaling function*. Indeed, as we shall see in the next Section, in the RFG the function f loses any dependence on both k_F and q, namely, one has superscaling in the non-Pauli-blocked regime. It remains to be seen what happens in the BCS model, *i.e.*, in the presence of correlations.

3 The RFG model and its BCS-inspired extension

Before presenting our model for the correlated system, let us shortly recall the Fermi gas result. The key tool for exploring superscaling is the nuclear spectral function $S(p,\mathcal{E})$. In the RFG model this reads [5, 6]

$$S^{RFG}(p,\mathcal{E}) = 4\,\theta(k_F - p)\delta(\mathcal{E} - T_F + T_p)\frac{V_A}{A(2\pi)^3}\,, \tag{6}$$

where $T_p = E_p - m_N$ is the struck nucleon kinetic energy, A the number of nucleons and V_A the volume enclosing the system. The integral (5) yields the RFG superscaling function [7]

$$f_{RFG}(\psi) = \frac{3}{4}\left(1-\psi^2\right)\theta\left(1-\psi^2\right)\,, \tag{7}$$

which depends only on one variable, defined as follows

$$\psi = \frac{1}{\sqrt{\xi_F}} \times \frac{\lambda - \tau}{\sqrt{(1+\lambda)\tau + \kappa\sqrt{\tau(1+\tau)}}}\,, \tag{8}$$

with $\xi_F = T_F/m_N$, $\kappa = \frac{q}{2m_N}$, $\lambda = \frac{\omega}{2m_N}$ and $\tau = \kappa^2 - \lambda^2$.

As outlined in the Introduction, we now extend the RFG model in order to account for NN correlations by assuming for both the initial ground state ($|BCS>$) and the daughter nucleus ($|D(p)>$) a BCS-like wave function, namely

$$|BCS> = \prod_k (u_k + v_k a^\dagger_{k\uparrow} a^\dagger_{-k\downarrow})|0> \tag{9}$$

$$|D(p)> = \frac{1}{|v'_p(p)|}\, a_{p\uparrow} \prod_k [u'_k(p) + v'_k(p) a^\dagger_{k\uparrow} a^\dagger_{-k\downarrow}]|0>\ . \tag{10}$$

In the above $|0>$ is the true vacuum and the states are correctly normalized providing $|u_k|^2 + |v_k|^2 = 1$ and $|u'_k(p)|^2 + |v'_k(p)|^2 = 1$. Note that the (u, v) and (u', v') coefficients are a priori different from each other: this point is of crucial relevance for our model, as we shall see below.

With the assumption (9) we have a covariant approximation to the nuclear ground state wave function. We have required that the added pairs always occur with back-to-back momenta (hence the net linear momentum of the system in its rest frame is zero) and with opposite helicities (hence the net spin of the ground state is zero). The creation operators add particles with relativistic on-shell spinors.

As is well-known, the states (9) and (10) do not correspond to a fixed number of particles, since they are not eigenstates of the operator $\hat{n}(k) = \sum_s a^\dagger_{ks} a_{ks}$. However we can compute the expectation values

$$n_{BCS}(k) = < BCS|\hat{n}(k)|BCS >= |v_k|^2 \tag{11}$$

$$n_{D(p)}(k) = < D(p)|\hat{n}(k)|D(p) >= |v'_k(p)|^2(1 - \delta_{kp}) \; . \tag{12}$$

and require the particle number (A for the initial state and $A - 1$ for the daughter nucleus) to be conserved on the average, which implies the conditions

$$\sum_k |v_k|^2 = A \, , \qquad \sum_{k \neq p} |v'_k(p)|^2 = \sum_k |v'_k(p)|^2 - |v'_p(p)|^2 = A - 1 \; . \tag{13}$$

Concerning the energy, we view our system as being constructed in terms of independent quasi-particles, writing accordingly

$$E_{BCS} = < BCS| \sum_{ks} E_k a^\dagger_{ks} a_{ks} |BCS >= \sum_k E_k |v_k|^2 \tag{14}$$

$$\begin{aligned} E_{D(p)} &= < D(p)| \sum_{ks} E_k a^\dagger_{ks} a_{ks} |D(p) >= \sum_{k \neq p} E_k |v'_k(p)|^2 \\ &= (E_{BCS} - m_N) - T_p |v_p|^2 + \sum_{k \neq p} T_k \left[|v'_k(p)|^2 - |v_k|^2 \right] \; , \end{aligned} \tag{15}$$

where in the last equation the constraints (13) have been exploited.

Before computing the spectral function, let us write down the expressions for the normalization conditions (13) in the thermodynamic limit $A \to \infty$, $V_A \to \infty$, $A/V_A = \rho_A$, $(A-1)/V_{A-1} = \rho_{A-1}$, namely

$$\lim \frac{1}{V_A} \sum_k |v_k|^2 = \int \frac{d^3k}{(2\pi)^3} |v(k)|^2 = \rho_A \; , \tag{16}$$

$$\lim \frac{1}{V_{A-1}} \left[\sum_k |v'_k(p)|^2 - |v'_p(p)|^2 \right] = \int \frac{d^3k}{(2\pi)^3} |v'(k;p)|^2 = \rho_{A-1} \; . \tag{17}$$

Assuming now $\rho_{A-1} = \rho_A \equiv \rho$ clearly entails $v'^2(k;p) = v^2(k)$, which allows us to drop the last term in (15). It must be emphasized that the coefficients v and v'

become identical in the thermodynamic limit, but are different for finite A. Hence it is crucial to compute the nuclear energies when A is finite and *then* take the thermodynamic limit.

We can then proceed to compute the daughter nucleus spectral function

$$S^{BCS}(p,\mathcal{E}) = |< D(p)|a_{p\uparrow}|BCS >|^2 \, \delta\left[\mathcal{E} - \left(E_{D(p)} - E_{D(k_F)}\right)\right] \frac{V_A}{A(2\pi)^3} \, , \tag{18}$$

where $E_{D(k_F)}$ is the energy $E_{D(p)}$ of the daughter nucleus evaluated at that value of p where it reaches its minimum, to be referred to as k_F in the BCS model:

$$\left.\frac{dE_{D(p)}}{dp}\right|_{p=k_F} = 0 \, . \tag{19}$$

Hence we have, after taking the thermodynamic limit,

$$\mathcal{E}(p) = E_{D(p)} - E_{D(k_F)} = T_F|v(k_F)|^2 - T_p|v(p)|^2 \, . \tag{20}$$

The matrix element in (18) can be straightforwardly computed, yielding $|v(p)|^2$,. Thus we end up with the expression

$$S^{BCS}(p,\mathcal{E}) = |v(p)|^2 \delta\left(\mathcal{E} - T_F|v(k_F)|^2 + T_p|v(p)|^2\right) \frac{1}{(2\pi)^3\rho} \, . \tag{21}$$

Finally, in order to calculate the superscaling function (5) what remains to be specified is the integration region Σ, which in turn requires knowledge of the separation energy. In the present model the latter turns out to be $E_s = -T_F|v(k_F)|^2$.

The last ingredient needed to calculate f are the coefficients $v(k)$ appearing in the BCS wavefunction. Although in principle these could be computed self-consistently, together with the energies E_k, starting from a model Hamiltonian, here we take a more phenomenological approach, choosing the following three-parameter expression

$$v^2(k) = \frac{c}{e^{\beta(k-\tilde{k})} + 1} \, . \tag{22}$$

Moreover, for sake of simplicity, we make the assumption $E_k = \sqrt{k^2 + m_N^2}$, namely we take the same single particle energies as in the RFG.

Next we use the constraints (16) and (19) to fix the parameters c and $\tilde{k}$, obtaining

$$c(\beta,\tilde{k}) = -\pi^2\beta^3\rho/Li_3\left(-e^{\beta\tilde{k}}\right) \tag{23}$$

and

$$\tilde{k} = k_F + \frac{1}{\beta}\log\left[\frac{\beta}{k_F}\sqrt{k_F^2 + m_N^2}\left(\sqrt{k_F^2 + m_N^2} - m_N\right) - 1\right] \, . \tag{24}$$

As far as the parameter β is concerned, it clearly controls both the modifications of the momentum distribution near the Fermi surface (promotion of pairs due to residual NN interactions, both long- and short-range) and also the tail of the momentum distribution due to short-range NN correlations. Indeed, for β very large

one recovers the familiar θ-distribution of the RFG, while for smaller and smaller β more and more particles are pulled out of the Fermi sea and produce a significant tail for the momentum distribution at large momenta. The impact of the physics expressed by the parameter β on the superscaling function is explored in the next section.

4 Results

In presenting the results obtained using our model it is convenient to start by displaying the behaviour of the parameters $\tilde{k}$ and c, which are fixed by the physical conditions of normalization and stability, versus β for given k_F. When $\tilde{k}$, c and β are known so are the wave functions of the initial and final nuclei.

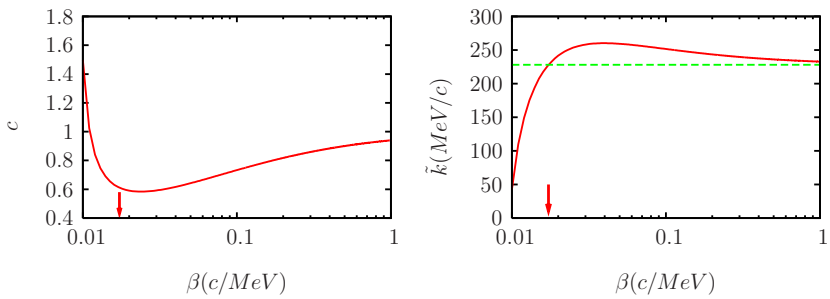

Figure 1. The parameters c and $\tilde{k}$, given in (23) and (24), respectively, shown as functions of β for $k_F = 228$ MeV/c and $\rho = k_F^3/(6\pi^2)$. The arrow indicates the critical value $\beta_{\rm crit} = 0.017$ c/Mev and the horizontal line in panel a corresponds to the Fermi momentum k_F.

In Fig. 1 the parameters $\tilde{k}$ and c are plotted versus β. For large β they stay constant (in fact the almost constant value of $\tilde{k}$ is quite close to the input value $k_F = 228$ MeV/c) until a critical value $\beta_{\rm crit} = 0.017$ c/MeV is reached where c ($\tilde{k}$) displays a dramatic increase (decrease). This value corresponds to the change of sign of the logarithmic term in (24), namely $\beta_{\rm crit} = \frac{2k_F}{T_F(T_F+m_N)}$. Thus our results appear to point to the existence of a narrow domain of β around $\beta_{\rm crit}$, below which the system becomes strongly disrupted by correlations. This has a strong impact on the structure of the superscaling function, as we shall see later.

In Fig. 2 we display the momentum distribution (11) of the initial nucleus for a few values of β larger (a) or smaller (b) than $\beta_{\rm crit}$. The progressive development of a tail in the momentum distribution is clearly seen in the figure: for values of β lower than $\beta_{\rm crit}$ the nuclear momentum distribution becomes very much extended beyond the Fermi sphere associated with the input value of k_F.

The next issue to be addressed is to determine where the spectral function is nonzero in the $(\mathcal{E}, p)$ plane. The answer is found in Fig. 3 where the support of the

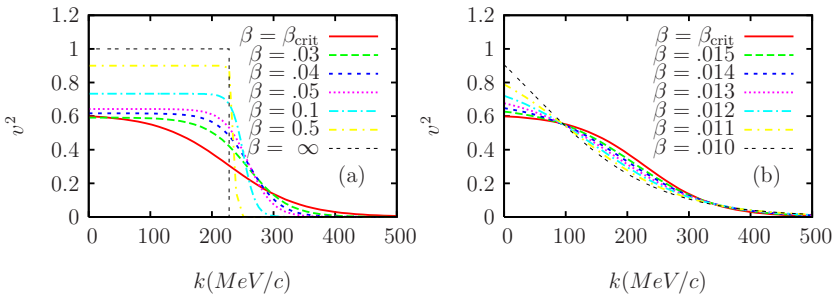

Figure 2. Momentum distribution of the initial state, Eq. (22), evaluated for $k_F = 228$ MeV/c, $\rho = k_F^3/(6\pi^2)$ and different values of β (in c/MeV) above (a) and below (b) the critical value $\beta_{\rm crit}$.

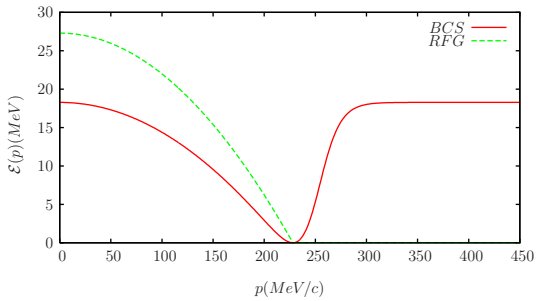

Figure 3. The excitation energy $\mathcal{E}$ computed according to (20) neglecting the last two terms for $k_F = 228$ MeV/c, $\rho = k_F^3/(6\pi^2)$, $\beta = 0.1$ c/MeV. The RFG results are also shown for comparison.

spectral functions of the RFG and of our BCS-inspired model are displayed and compared. Both spectral functions of course are just δ-functions, but concerning their support two major differences distinguish the two: 1) in the range of momenta where both exist the excitation spectrum of the daughter system is substantially softer than the RFG one; 2) for missing momenta larger than k_F the BCS case, unlike the RFG, continues to display a spectrum, which in the thermodynamic limit rises quite suddenly with p until it reaches the value $\mathcal{E}$ assumes for vanishing missing momentum, namely $\mathcal{E}_{\rm max} = T_F|v(k_F)|^2$. This energy is reached only at $p = \infty$, but over a large span of momenta $\mathcal{E}$ remains almost constant, thus corresponding to the situation of an eigenvalue with infinite degeneracy stemming from the symmetry $U(1)$ associated with the particle number conservation. As p is lowered, approaching the Fermi surface, the degeneracy is lifted and we face a situation of a spontaneously broken symmetry, reflected in the structure of our state which contains components of all possible particle number. This situation is strongly reminiscent of superconductivity, where the spontaneous symmetry breaking also occurs in the proximity of the Fermi surface.

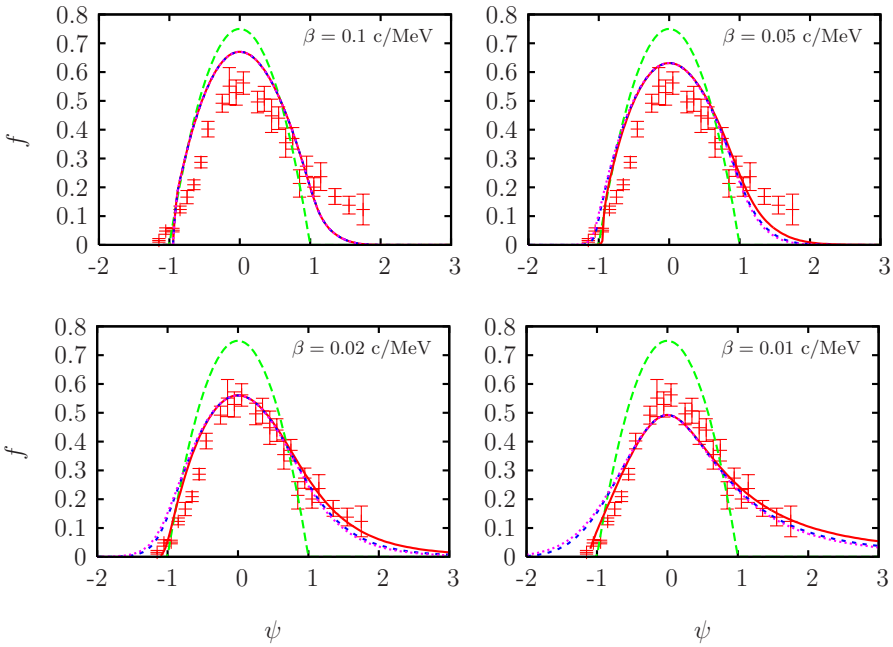

Figure 4. The superscaling function f defined in (5) plotted versus the scaling variable (8) in the RFG model (green) and in the present BCS model for three values of q (red: 500 MeV/c, blue: 1000 MeV/c, magenta: 1500 MeV/c) and different values of β. As usual, k_F =228 MeV/c. Data are taken from [8, 9].

This set of degenerate states has a dramatic impact on the superscaling function f, which is displayed in Fig. 4 versus the scaling variable ψ for a few values of β and q. For comparison the RFG result in (7) and the averaged experimental data [8, 9] are also shown. One sees that to get f for large positive ψ we have to integrate in the $(\mathcal{E}, p)$ plane in domains encompassing large fractions of those degenerate states discussed above. These are thus the cause of the asymmetry of the scaling function with respect to $\psi = 0$ appearing in Fig. 4. For ψ large and negative these states are to a large extent excluded from entering into the building up of f. The fact that this effect is more and more pronounced as β becomes smaller reflects the impact of the tail of the momentum distribution which indeed grows when β decreases and, as a consequence, more degenerate states participate to build up f. Note that values of β around the critical value yield a tail which is in qualitative agreement with the experimental data.

As far as scaling of the first kind is concerned, Fig. 4 shows that this is quickly reached in the vicinity of the QE peak, although not so to the right and to the left of it. A closer examination of the results (see Fig. 5, where f is plotted on a logarithmic scale for a wider q-range at β=0.01 c/MeV) shows that also here the BCS model does scale, however with an onset reached only for $q \simeq 1.5$ GeV/c, namely for

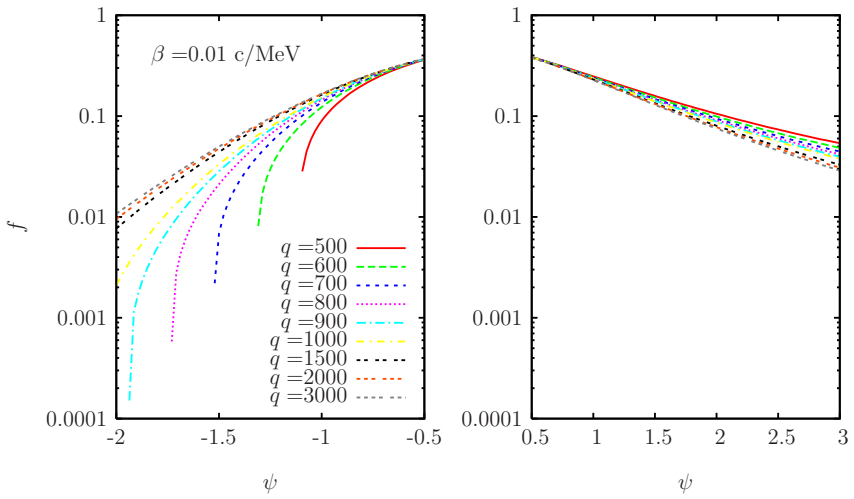

Figure 5. The superscaling function f in the negative ψ region plotted for several values of q (in MeV/c) and $\beta = 0.01$ c/MeV. As usual, k_F =228 MeV/c.

larger momenta than when at the QE peak where the onset already occurs at about 500 MeV/c. Also from Fig. 5 it appears that the scaling regime is reached faster to the right than to the left of the QE peak. Moreover, the asymptotic value for $\psi < 0$ is approached from below, namely the superscaling function grows with q until it reaches its asymptotic value, in contrast with the experimental findings. This reflects the fact that our model, although appealingly simple, is not able to account for features of this kind. Note that the same trend of approaching first-kind scaling from below is also found within the framework of the Coherent Density Fluctuation Model [10] where realistic nucleon momentum and density distributions are used [11]. On the other hand, in relativistic mean-field theory [12] the approach is from above, and thus in better accord with the experimental data.

Finally, using the present BCS model, we investigate the second-kind scaling behaviour, namely the dependence of the function f upon the nuclear species. Following the original procedure of Refs. [3], we choose for each nuclear species a momentum k_A (which is a phenomenological parameter, not necessarily coinciding with the Fermi momentum as it must reflect both initial- and final-state interaction effects) and use it in the definition (8) of the scaling variable ψ and of the dividing factor (4). For simplicity, in the present approach the value of k_A is chosen in order to have all the corresponding superscaling functions coincide at the QE peak, thus realizing superscaling at least where the nuclear response is the largest. The results are displayed in Fig. 6, where each curve corresponds to given k_F and k_A. Over much of the range of ψ shown in the figure one sees relatively good second-kind scaling, although the results still point to a sizable violation of the second kind scaling in the scaling domain (large negative ψ).

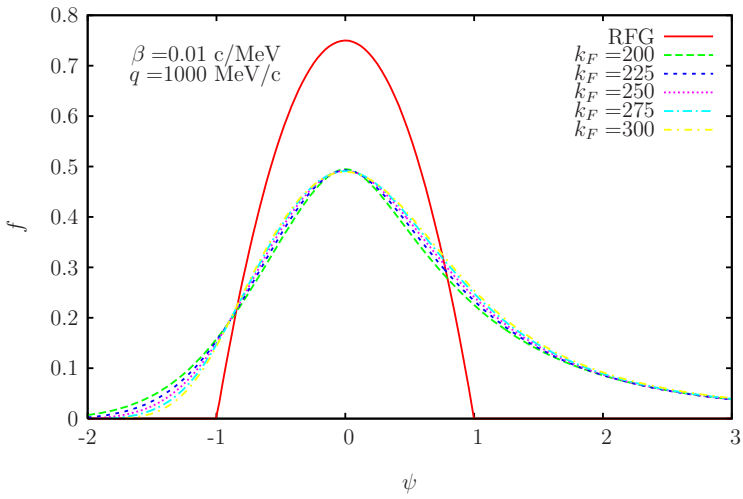

Figure 6. The superscaling function f plotted versus ψ for several values of the Fermi momentum k_F (in MeV/c) and with k_A devised in such a way that the peaks coincide (see text).

5 Conclusions

In the present study a simple extension of the relativistic Fermi gas model for studies of relatively high-energy inclusive electroweak cross sections has been developed. Starting from the RFG in which a degenerate gas of nucleons is assumed for the nuclear ground state, in this extension pairs of particles are promoted from below the Fermi surface to above, yielding a spectral function and the resulting momentum distribution with Fourier components for all values of momentum. In the spirit of the RFG this new model has been constructed in a way that maintains covariance.

To summarize our findings, we have shown that, likely because in the BCS spirit we limit ourselves to an independent quasi-particle description of nuclear matter, scaling of the first kind (independence of momentum transfers q) appears to occur not only at the QE peak, but also at both lower and higher energy transfers ω. We found that the onset of first-kind scaling already occurs at momentum transfers of order 500 MeV/c at the QE peak, whereas away from the QE peak the onset only occurs at quite large momentum transfers (of the order of 2 GeV/c). Furthermore, the shape of the superscaling function turns out to be *non-symmetric* around the QE peak, being larger to the right and smaller to the left of it, namely, in agreement with experiment and thus lending support to our approach. However, in our model when in the so-called scaling region (below the QE peak) first-kind scaling is reached as a function of q from below, which is not what is experimentally found. Finally, scaling of the second kind (independence of nuclear species) is shown to be relatively well satisfied, given that an appropriate momentum scale is chosen for each nuclear species, although some violations appear for large negative ψ.

References

1. J. E. Amaro, M. B. Barbaro, J. A. Caballero, T. W. Donnelly, A. Molinari and I. Sick, Phys. Rev. C **71**, 015501 (2005).
2. D. B. Day, J. S. McCarthy, T. W. Donnelly and I. Sick, Ann. Rev. Nucl. Part. Sci. **40**, 357 (1990).
3. T.W. Donnelly and I. Sick, Phys. Rev. Lett. **82**, 3212 (1999); Phys. Rev. C **60**, 065502 (1999).
4. M. B. Barbaro, R. Cenni, T. W. Donnelly and A. Molinari, Phys. Rev. C **78**, 024602 (2008).
5. R. Cenni, T. W. Donnelly and A. Molinari, Phys. Rev. C **56**, 276 (1997).
6. M. B. Barbaro, R. Cenni, A. De Pace, T. W. Donnelly and A. Molinari, Nucl. Phys. A **643**, 137 (1998).
7. W. M. Alberico, A. Molinari, T. W. Donnelly, E. L. Kronenberg and J. W. Van Orden, Phys. Rev. C **38**, 1801 (1988).
8. C. Maieron, T. W. Donnelly and I. Sick, Phys. Rev. C **65**, 025502 (2002).
9. J. Jourdan, Nucl. Phys. A **603**, 117 (1996).
10. See M. Ivanov, this workshop.
11. A. N. Antonov *et al.*, Phys. Rev. C **74**, 054603 (2006); Phys. Rev. C **73**, 047302 (2006); Phys. Rev. C **69**, 044321 (2004).
12. J. A. Caballero, J. E. Amaro, M. B. Barbaro, T. W. Donnelly, C. Maieron and J. M. Udias, Phys. Rev. Lett. **95**, 252502 (2005).